Oil & Gas Science and Technology – Rev. IFP, Vol. 58 (2003), No. 6, pp. 667-683

X-Ray Absorption Spectroscopy and Anomalous Wide Angle X-Ray Scattering: Two Basic Tools in the Analysis of Heterogeneous Catalysts

D. Bazin[1], J. Lynch[2] and M. Ramos-Fernandez[2]

1 LURE, Université Paris XI, Bât. 209D, 91898, Orsay - France
2 Institut français du pétrole, Physics and Analysis Division, 1 et 4, avenue de Bois-Préau, 92852 Rueil-Malmaison Cedex - France
e-mail: john.lynch@ifp.fr - dominique.bazin@lure.u-psud.fr - martam.ramos@yahoo.com

Résumé — Spectroscopie d'absorption et diffusion anomale à grands angles des rayons X : deux outils de base dans l'analyse de catalyseurs hétérogènes — Notre compréhension des processus physicochimiques à l'échelle atomique dans des nanomatériaux a progressé de manière notoire ces dernières décennies grâce à l'émergence de techniques liées au rayonnement synchrotron. Dans cet article, nous décrivons la spectroscopie d'absorption des rayons X mous et durs et la diffusion anomale des rayons X, deux techniques se servant des propriétés spécifiques d'un faisceau synchrotron, en particulier de la large gamme spectrale. Nous centrons la présentation sur les avancées dans la description de catalyseurs hétérogènes. Les apports et les limitations de chaque technique sont analysés.

Abstract* — *X-Ray Absorption Spectroscopy and Anomalous Wide Angle X-Ray Scattering: Two Basic Tools in the Analysis of Heterogeneous Catalysts — *In the past decades, our understanding of physico-chemical processes at the atomic level in nanomaterials has been significantly improved by the emergence of synchrotron radiation related techniques. In this review paper, we describe two techniques: X-ray absorption spectroscopy (XAS) using soft and hard X-rays, and anomalous wide angle X-ray scattering (AWAXS), both of which use some of the specific properties of a synchrotron beam, in particular the wide spectral range. We focus on the numerous breakthroughs which have been achieved using these techniques in describing heterogeneous catalysts. The merits and shortcomings of each technique are discussed.*

INTRODUCTION

Our understanding of heterogeneous catalysis at the atomic level is developing rapidly at the present time [1-8], this particular family of materials being implied in major environmental challenges of our modern society such as the NOx removal processes [9].

From a theoretical standpoint [10-13], many of the numerous new insights gained in this field are due to the possibility to describe in a realistic way the electronic structure of nanometer scale entities [14-17] and thus to understand both their atomic and chemical rearrangements [18, 19].

From an experimental point of view, the emergence of synchrotron radiation methods [20, 21] gives the required abilities to characterise such nanomaterials during the chemical reaction [22, 23]. The use of *in situ* analysis cells enables a detailed description of catalyst structure in reactive atmospheres and opens the possibility of correlating structure with catalytic activity [24]. This research field has repeatedly attracted the attention of major industrial research groups like *PSA* [25], *Elf* [26], *DSM* [27], *Shell* [28, 29], *Rhodia* [30], *Total* [31, 32], *Mobil* [33], or *Exxon* [34].

Photon-matter interaction occurs via two fundamental channels: absorption (the energy of the photon is lost within the target) and scattering processes which can be either elastic (Thomson scattering for free electrons) or inelastic (Compton scattering). Note that the interaction of photons with nuclei is out of the X-ray range considered here (between 3 to 25 KeV). The particular properties of synchrotron radiation such as the wide spectral range and the exceptional flux have led to the development of various techniques such as X-ray absorption spectroscopy (XAS) using either soft [35] and hard X-rays as well as anomalous wide angle X-ray scattering (AWAXS) [36, 37].

Heterogeneous catalysts, and in particular industrials catalysts present a large degree of variety in terms of composition, structure, required functions [38, 39]. They range from zeolites [40, 41], CeO_2 [42], C [43], ZrO_2 [44, 45] or TiO_2 [46] and mixed oxides (such as Al_2O_3-CeO_2 [47] or WO_3-CeO_2 [48]) to metals (Fe [49], Co [50], Cu [51], Zn [52], Nb [53], Ru [54], Pd [55, 56], Sn [57], W [58], Ir [59, 60], Pt [61, 62], Au [63]) and sulphides (Mo [64-67], Ni [68], Co [69], Nb [70]) supported by oxides.

Laboratory characterisation techniques, such as transmission electron microscopy, *in situ* XRD [71] or FTIR [72] contribute to a description of the solids but do not precisely show the structure of nanometer scale particles. A combination of several characterisation techniques is necessary to obtain a coherent description of these solids. In summary, if laboratory techniques constitute a starting point for analysis, modern materials studies systematically integrate synchrotron radiation related techniques [73, 74].

In this review we illustrate, through a survey of recent literature illustrated by experimental results obtained in collaborative research by the *Laboratoire pour l'utilisation du rayonnement électromagnétique (LURE)* and the *IFP*, the information given by each of the techniques. The merits and shortcomings of each are discussed.

1 SOFT X-RAY ABSORPTION SPECTROSCOPY

Soft X-ray absorption spectroscopy exploits the so-called "near-edge X-ray absorption fine structure" (NEXAFS) also known as "X-ray absorption near-edge structure" (XANES) beginning before the absorption threshold, E_0, and continuing up to about 40 eV after the edge.

Soft X-ray absorption spectroscopy (for a detailed description see references [75, 76]) has proved to be a very powerful tool in different disciples such as biology or magnetism [77] and more particularly in heterogeneous catalysis [78-80]. Recent advances in the theoretical analysis as well as in the instrumentation [81, 82] have motivated several studies dedicated to the application to heterogeneous catalysts of X-ray absorption spectroscopy at low energy [83-89].

The new approach allows experiments at the K edge of light elements *e.g.* carbon, nitrogen, oxygen [90, 91] or sulphur [92] and/or at the L edges of 3d transition metals [93, 94].

For the transition metals which constitute the metallic part of the catalyst, weak structures such as a shoulder are generally observed in the spectrum at the K edge (3d and 4d transition metals), whereas very fine structures are present at the L and M edges. The observation of such fine details associated with the emergence of a coherent theoretical formalism allows a more precise description of the structural and electronic characteristics of this family of materials compared to that obtained through more classical EXAFS based on hard X-ray photons. Moreover, since X-ray absorption spectra can also be collected at the K edge of light elements, the adsorption process of molecules of major interest in heterogeneous catalysis can be studied completely, seen from viewpoint of the two actors of the chemical bond. This leads to a more precise knowledge of intermediate species. For instance, adsorption of light molecules (CO, NO, O_2, etc.) on metals can now be characterised by studying simultaneously the molecule itself and the metal atoms.

1.1 Experimental Set-Up and Experimental Limitations

Soft X-ray absorption spectroscopy is implemented at several synchrotron radiation centres. Among these, a new soft X-ray (50-1500 eV) beamline has been constructed at a bending magnet station at the *Photon Factory* in order to perform photoemission spectroscopy (PES), X-ray absorption fine structure (XAFS), and photoelectron diffraction (PED) experiments in surface chemistry [95].

At *LURE*, soft X-ray spectroscopy measurements dedicated to heterogeneous catalysis can be carried out on three different beamlines. Beamline "SA32", using a focusing toroidal mirror and total electron yield detection [96, 97] is implemented on the "*SACO*" ring with an available energy range of 0.8 to 4 keV. A double crystal monochromator (fixed exit) made of beryl, quartz or InSb, can be used depending on the element of interest. The energy range may be limited by the composition of the crystals (as is the case for collection at the K edge of Mg and Al using beryl or quartz).

Also on *SACO*, the beamline "SACEMOR" [98] placed after a bending magnet is equipped with a high-resolution spherical mirror-plane grating monochromator (12 m, 200-800 eV). The monochromator resolution is about 0.15 eV for the cobalt L_{III} edge. Beam dimensions are about 0.5 mm × 0.2 mm at the sample *(Fig. 1)* and the pressure in the analyser chamber is directly related to the vacuum in the synchrotron ring.

The K edge spectra of light elements such as sulphur can be obtained at *LURE* on the D44 station *(Fig. 2)* of the *DCI* storage ring, typically running at 1.85 GeV with an average current of 300 mA and a lifetime of 200 h. X-rays are monochromatized by two Si (111) monocrystals. The incident I_0 and transmitted I_1 intensities are recorded by use of two ionisation chambers.

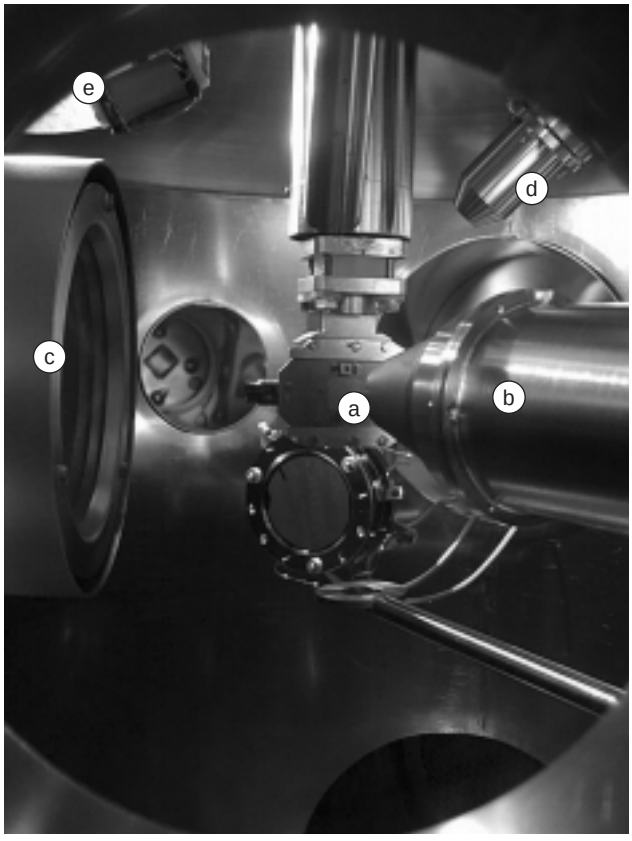

Figure 1

Internal view of the acquisition chamber of the SACEMOR experiment implemented on *SACO*.
a) sample; b) electron analyser; c) low energy electron diffraction detector; d) quadrupole mass spectrometer; e) total electron yield detector.

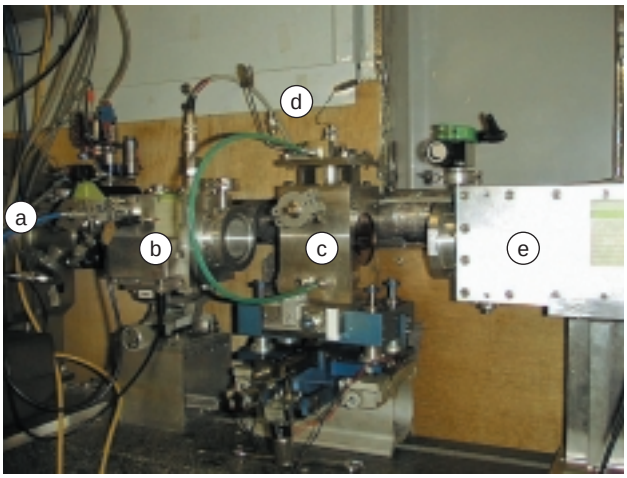

Figure 2

Partial view of the D44 beamline implemented on *DCI*. a) synchrotron beam; b) ionisation chamber to measure the intensity before the sample; c) reaction cell; d) gas arrival and exit lines; e) ionisation chamber to measure the intensity after the sample.

In some respects, soft X-ray spectroscopy offers the possibility to perform *in situ* experiments. However, if the temperature of the sample as well as the nature of the reactive gas can be considered as "free" parameters, this is definitely not the case of the pressure. The pressure in the sample environment during the experiment has to be compatible with the low energy of the incident photon (as well as, for emission measurements, with the energy of the photons/electrons coming from the sample). This imposes a limitation on the value of the gas pressure during the experiment of approximately 10^{-10} Pa. High pressure experiments ($p > 20$ bar) can be carried out in a preparation chamber, the catalyst being then transferred. As we will demonstrate, this technique enables a real improvement in the knowledge of the structural evolution of the material in reaction conditions.

1.2 Nitrogen K-Edge Studies of the Adsorption of NO on Nanometer Scale Metallic Oxide Particles

The adsorption of NO on supported Pt/Al_2O_3 was studied by NEXAFS at the nitrogen K edge [99]. Prior to NO adsorption, carbon K-edge and nitrogen K-edge spectra were measured on the catalyst in order to evaluate a possible contamination of the sample. The Pt/Al_2O_3 catalyst was exposed to O_2 gas and then to NO during 10 min at 10^{-6} Pa. The absorption spectrum collected at the nitrogen K edge is shown in Figure 3. Thus, the information regarding the adsorption mode of a molecule on a real catalyst, is available.

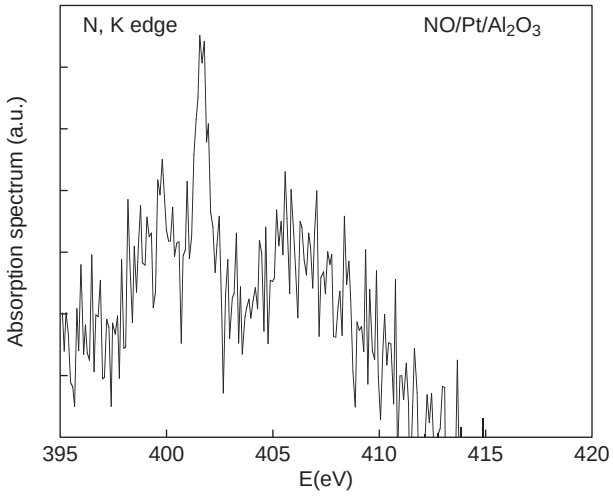

Figure 3

Nitrogen K edge absorption spectrum collected after the adsorption of NO on a Pt/Al_2O_3 catalyst.

1.3 The Sulphur K Edge: Environment of Sulphur in Organic Compounds

Sulphur K-edge XANES provides a fingerprint of the forms of sulphur present in organic compounds [100, 101]. However, the analysis of solids containing a mixture of different types of sulphur is difficult. Kerogenes may contain a large range of sulphur types such as FeS, FeS_2, organic sulphides, thiophenic sulphur, oxidised organic sulphur and sulphates [102, 103].

Waldo *et al.* [104] established a relationship between the white line intensity measured at the sulphur K edge and the position in energy, which can be used to determine the distribution of sulphur amongst the different possible forms. Following this approach *(Fig. 4)*, kerogene samples have been characterised at different stages of a pyrolysis experiment. The initial broad white line around 2473 eV indicates the presence of both thiophenic and bridging sulphur content. After heating to 550 K the white line appears sharper and at higher energy (bridging sulphur bonds have been broken) and the absorption edge begins at lower energies suggesting formation of additional mineral sulphide (FeS_2). On further heating this sulphide in turn decomposes to FeS, liberating more sulphur. Thus, information on the distribution of sulphur among the different forms is available through this simple method [105].

1.4 The L Edge of 3d Elements

Preparation of the PdCo and RuCo samples has been fully described in earlier papers [106-108]. The Co L_{III} edge of $CoPd/SiO_2$ and $CoRu/SiO_2$ catalysts has been followed during reduction and CO adsorption. Figure 5 shows the case for the CoPd solid. In the initial state of the bimetallic $CoRu/SiO_2$ catalyst, the shape of the L_{III} edge shows the presence of Co_3O_4 clusters (very similar to the monometallic Co/SiO_2 case). On reduction, the Co L_{III} edge is modified then, after CO adsorption, an edge spectrum corresponding to the spectra obtained for the $SiCo_2O_4$ reference compound is observed. It is thus clear that Co atoms are in the Co^{2+} (O_h) electronic state.

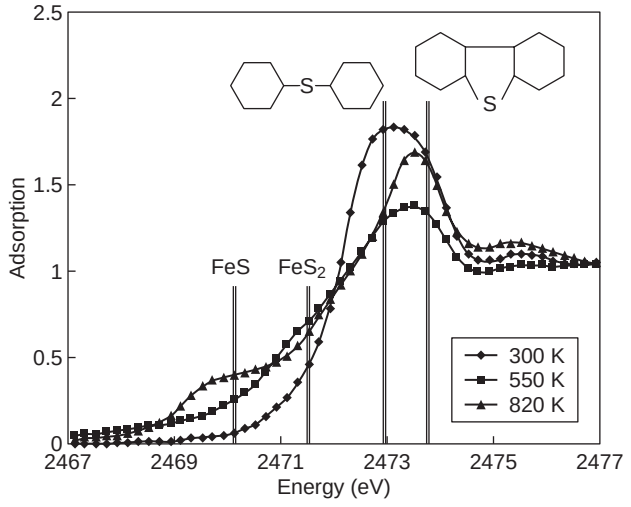

Figure 4

White line intensity measured at the sulphur K edge of kerogen sample as a function of temperature.

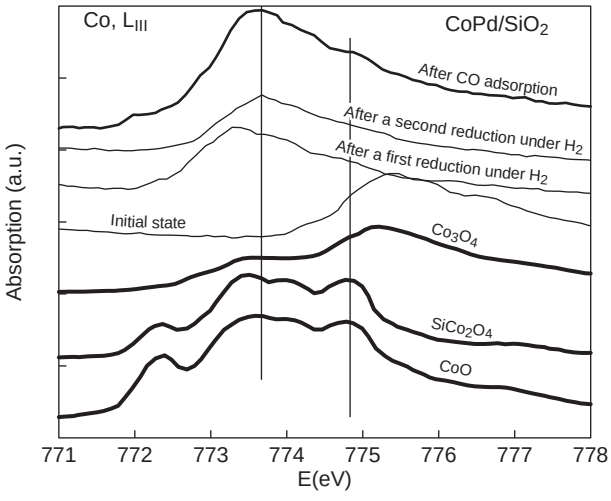

Figure 5

Evolution of the Co L_{III} edge after *in situ* reduction and *in situ* CO adsorption.

Information regarding the structural and electronic environment of metals of a real catalyst is thus available.

2 HARD X-RAY ABSORPTION SPECTROSCOPY

For high energy X-ray photons the details of the XANES part of the absorption spectrum are less detailed, making extraction of quantitative information difficult. Important information may however be obtained on the local structure around an element from the "extended X-ray absorption fine structure" (EXAFS: from E_0 + 40 eV to E_0 + 1500 eV).

The basic model is the following: the absorption of an X-ray photon by an atom ejects a photoelectron, which is scattered by neighbours. An interference process builds up between the wave function of the outgoing electron and its scattered parts, leading to a modulation of the absorption coefficient. Far beyond the absorption edge, the electron is assumed to be free. The scattering is weak and involves only one neighbour atom (single scattering approximation).

2.1 Experimental Set-Up

As stated previously, X-ray absorption spectroscopy now constitutes a basic chemical analysis tool. Thus, each new third generation synchrotron radiation centre has developed one or several beamlines dedicated to X-ray absorption spectroscopy [109]. Often these beamlines offer the possibility either to collect a diffraction diagram at the same time [110-115] or to follow in real time a chemical reaction [116-120].

At *LURE*, this type of facility has been implemented on two beamlines: H10 and the dispersive experiment, both of which will be transferred on the new French synchrotron radiation centre *SOLEIL* [121-123].

H10 *(Fig. 6)* is a new beamline for materials studies [124] implemented at DCI based on the complementary aspect of different techniques specific to synchrotron radiation. X-ray diffraction (XRD) and XAS are both feasible, in the 4 to 20 keV range. XAS as well as XRD are carried out in the monochromatic mode, using a fixed exit Si (111) double crystal monochromator. Although XAS and XRD can not be measured exactly at the same time, the possibility to do both measurements consecutively without changing the set-up is an advantage when the samples are not very uniform or when it is important that the physical parameters, or the atmosphere are identical. This is often a concern when carrying out experiments on "real" materials, in particular using severe environmental conditions.

Beamline D11 (dispersive XAS, *Fig. 7*) is installed on the DCI positron storage ring (1.85 GeV) [125]. A dispersive bent triangular shaped crystal (Si 111) is used to focus the polychromatic X-ray beam (10^{10} photons s^{-1}) on to the sample. Then the beam diverges toward a position sensitive detector made of 1024 sensing elements (2500 μm high by 25 μm in width). The sample (a solid, a solution, or an electrode in the electrochemical cell) is aligned so that the focused X-ray beam, with an area of 0.2 cm^2, passes through it.

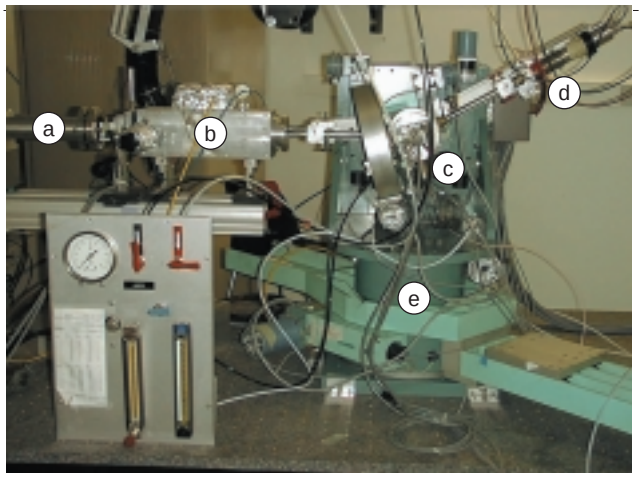

Figure 6

The H10 absorption-diffraction experiment implemented on *DCI*.
a) synchrotron beam; b) ionisation chamber to measure the intensity before the sample; c) reaction cell; d) fluorescence detector; e) 6 circle diffractometer.

For Pt foil, the acquisition time for one spectrum is a few seconds. In the transmission mode, the absorption is defined by ln (I_0/I), where I_0 and I are the incident and transmitted signals, respectively. Note that the presence of a single detector makes it necessary to carry out two different experiments, without and with the absorber element, to acquire the data necessary to extract the absorption spectra. When using the electrochemical cell, a sample identical to the real electrode, but without the active element, is used to record I_0. For catalysts the support alone can be used to record a background. These I_0 recordings allow the weakly energy-dependent absorption by other elements to be taken into account.

2.2 The L Edge of 5d Transition Metals

It is well known that information can be obtained on the electronic state of the absorbing atom by studying the white lines or threshold spikes which appear at the $L_{II,III}$ edges of the transition metals.

The L_{III} white line intensity depends on the electronic charge transfer between either the nanometer scale metallic particle and the support or between the two metals which are present inside the cluster. An early study by Lytle *et al.* [126] showed the effect of chemical environment on the magnitude

of L_{III} platinum white line. Numerous studies since have used the shape of the edge as a probe to determine the chemical state of the metal [127]. These studies can be performed after [128] or during a chemical reaction [129], the spectra being collected *in* or *ex situ*. In Figure 8, the white line intensity for a Pt/Al_2O_3 catalyst as a function of reduction temperature is converted into electron vacancy density by reference to the calculated values for platinum oxide and bulk metal. The slow decline to a value of 1 e^- per atom (the theoretical value for isolated Pt atoms) at 600 K is followed by a rapid reduction as metal particle formation occurs.

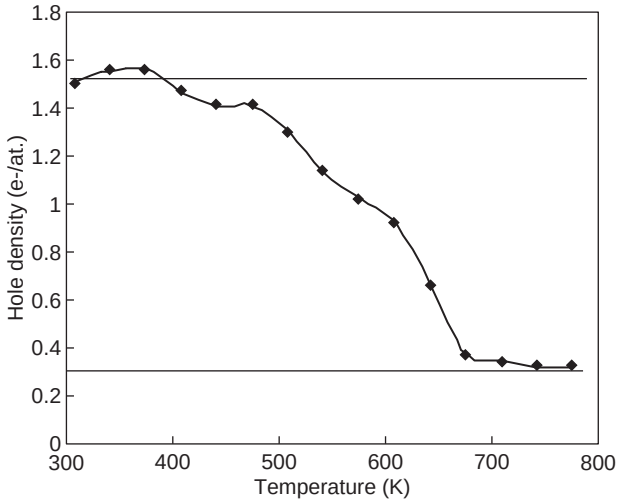

Figure 7

The density of electron vacancies as a function of reduction temperature for a Pt/Al_2O_3 catalyst. Horizontal lines refer to the values for PtO_2 and Pt bulk metal.

From a fundamental point of view, we have shown recently through *ab initio* calculations [130] that a strong correlation exists between the intensity of the white line and the size of the cluster. The intensity of the white line varies with the size of the cluster. Indeed, the density of states of a nanometer scale cluster being different from that of the bulk, one would expect the intensity of the white line to be different. Thus, in contrast with numerous studies which measure electronic transfer through a comparison with the white line of the platinum foil, we show that assuming charge transfer is not necessary to explain many of the variations of the white line intensity.

2.3 The K Edge of 3d and 4d Transition Metals

The XANES part of the K edge spectrum can be simulated with a linear combination of the XANES of well crystallised reference compounds. Such analysis, called PCA (principal component analysis) assumes that the absorbance in a set of spectra can be mathematically modelled as a linear sum of individual (uncorrelated) components known as factors [131, 132]. In the case of nanometer scale metallic cluster, particular attention has to be paid to the choice of reference compounds [133].

K-edge XANES spectra of most elements of the periodic table can also be simulated *ab initio*. Let us consider the near edge part of the absorption spectrum of copper foil which exhibits three main features *(Fig. 9)* α (1s to 4p transition in the $3d^{10}$ configuration which belongs thus to the NEXAFS part of the spectrum), β and γ. This face centred cubic (fcc)

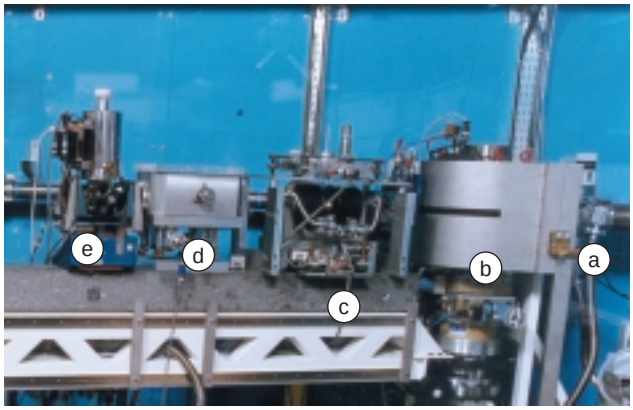

Figure 8

The dispersive experiment implemented on *DCI*.

a) white beam; b) dispersive monochromator; c) high pressure cell; d) silica mirror to remove harmonics; e) photodiode array detector.

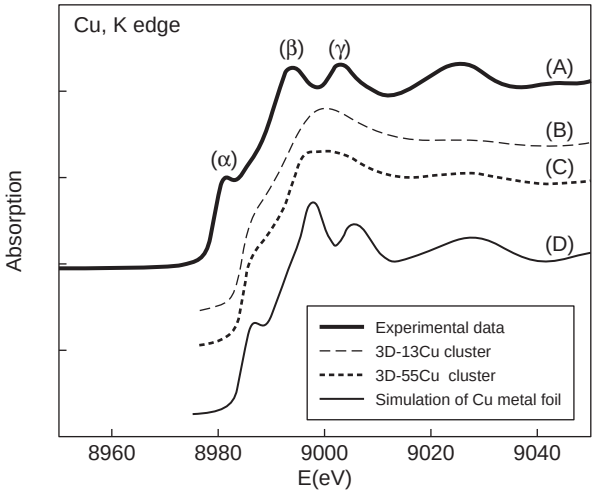

Figure 9

Near edge part of the K absorption edge as measured for the copper foil (A) and as calculated with the FEFF program for clusters of 13 atoms (B) and 55 atoms (C) of copper and a cluster of 200 atoms of copper (D).

lattice is generally reproduced in the multiple scattering framework in the muffin-tin approximation by using large clusters in which the absorbing atom is always at the centre of the cluster, the surface atom contribution to the total cross section being negligible.

In the case of a 13 atoms cluster, it is essential to consider each kind of atom in the cluster since the signal from the surface and from the central atom are significantly different. Clearly, a 13 atom environment is not enough to produce the resonance (γ). A similar calculation was made for a 55 copper atom cluster *(Fig. 9, curve C)*. The major point that has to be underscored is the presence of the features (β) and (γ) of the copper foil K edge [134]. The structure α, as expected, is also band structure dependent (and thus this feature is size dependent).

2.4 Extended X-Ray Absorption Fine Structure (EXAFS)

The relation between the modulated part $\chi(k)$ of an absorption spectrum and the structural parameters of the sample, has been established in numerous theoretical works [135, 136] and can be written as:

$$\chi(k) = \sum_j \left\{ \frac{N_j}{kR_j^2} \right\} f_j(k) \sin\left(2kR_j + \Phi_j(k)\right) \exp\left(\frac{-\Gamma(k)R_j}{k} \right) \exp\left(-2\sigma_j^2 k^2\right) \quad (1)$$

where k is the wave vector of the photoelectron, j refers to the different coordination shells at a distance R_j from the absorbing atom, each shell containing N_j equivalent atoms. A Debye-Waller factor σ_j takes into account the fact that a spread in distance exists in the material and we assume that this distribution is Gaussian. Generally, the electron mean free path $\Gamma(k)$ is introduced in order to reflect the probability that the electron is inelastically scattered by its environment. The backscattering amplitude $\Phi_j(k)$ is essentially the magnitude of the transform of the scattering potential and its shape is a measure of the type of scattering atom.

A Fourier transform (FT) of the EXAFS with respect to the photoelectron wave number will show peaks at distances corresponding to the nearest neighbour atomic coordination shells. Thus, between $\chi(k)$ and the radial distribution function around the central atom, there is a simple FT relationship on which the analysis procedure is based. Conventional analysis of the EXAFS modulations contains several well-known steps [137, 138]. The most important of these are: subtraction of the background absorption and normalisation, extracting the $\chi(k)$ function, the FT of $\chi(k)$ in order to obtain a pseudo radial distribution function and finally the curve fitting procedure in k-space to obtain the structural parameters. We have illustrated the importance of multiple scattering process, in the case of the Cu foil (K edge) as well as the Pt foil (L edge). Also, it is important to underline that EXAFS is insensitive to polydispersity.

In the case of Pt clusters, it is easy to build the EXAFS modulations *(Fig. 10)* as well as the FT modulus *(Fig. 11)*. These plots show that the EXAFS spectroscopy is suitable for very small clusters, the number of first neighbours varying rapidly in this size range but not for larger particles (*i.e.* clusters containing more than a thousand atoms) for

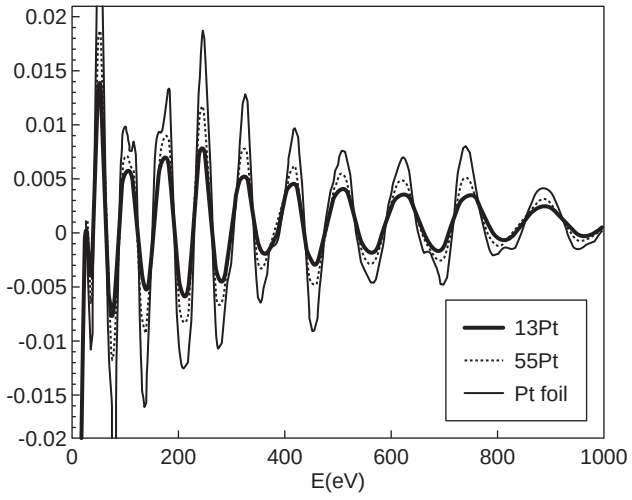

Figure 10

Variation of the EXAFS modulations *versus* the cluster size (dots: cluster of 13 (bold line) and 55 atoms; line: simulation of the metallic foil).

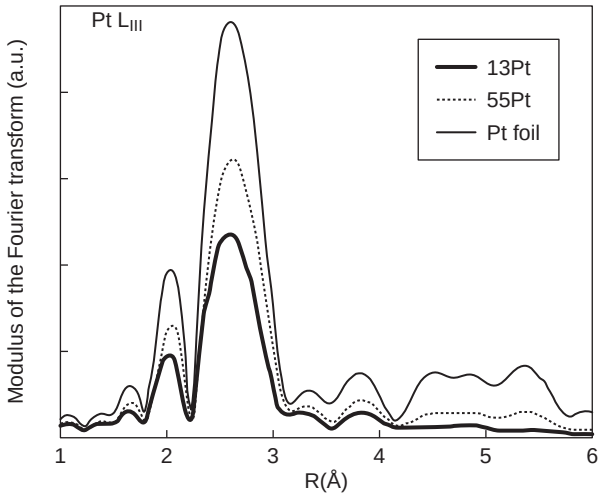

Figure 11

The Fourier transform modulus uncorrected for phase shift associated with clusters of 13 atoms (13Pt, bold line) and 55 atoms (55Pt, dots) of platinum compared to the modulus of a platinum foil (line).

which the FT modulus is very similar to the modulus of the platinum metallic foil. EXAFS spectroscopy is thus a structural probe, sensitive only to the local order (because of the mean free path term Γ) around one given type of atom in the sample (well defined by its X-ray absorption edge). This technique is now an invaluable tool for catalyst characterisation which can establish a link between the structural characteristics of the metallic part of the catalyst and its chemical activity.

One of the major successes of EXAFS spectroscopy has been obtained with the characterisation of the preparation steps of the catalysts. The most frequent preparation procedure includes three steps: impregnation-drying, calcination and reduction. Each has a major impact on the final structural characteristics of the material. For example, several studies have shown the importance of the choice of the precursor as well as the chlorine content during the impregnation steps [139]. Also, the temperature of calcination is determinant in the formation of heteroatomic bonds in the case of several bimetallic catalysts. Finally, the temperature and the time of reduction control the size of the metallic cluster finally generated [140-143].

Many of the bimetallic systems are easy to study due to the significant difference in the backscattering function of the different types of metal atom but this is not the case for systems such as Pt-Re [144] or Pt-Au [145] bimetallic catalysts. For these catalysts, one can use the proximity of the L edges of the two metals *(Fig. 12)* to follow "simultaneously" the evolution of their electronic states *(Fig. 13)* during reduction so as to obtain information on the formation of truly bimetallic particles [146].

3 ANOMALOUS WIDE ANGLE X-RAY SCATTERING (AWAXS)

In recent years, AWAXS experiments have been performed in several synchrotron radiation centres taking advantage of experimental improvements [147]. Various kinds of systems [148, 149] such as supported metallic clusters [150-152], Pt-Mo [153, 154], Pt-Re [155] catalysts or oxide compounds [156-159] have been investigated. For data analysis by direct comparison of calculated and experimental intensities, the first step is to set up a plausible model of the material and calculate the interatomic distances between all pairs of atoms [160]. The corresponding intensity is then calculated from the Debye formula as a function of scattering vector q and compared with the coherently scattered intensity observed experimentally. The model is refined until a satisfactory agreement is reached between the two curves.

3.1 The Associated Formalism

We recall here the basic elements associated with this technique [161-163]. AWAXS uses the energy dependence of the atomic scattering factor $f(q,E)$ near an absorption edge. This parameter is expressed in electron units as:

$$f(q,E) = f_0(q) + f'(E) + if''(E) \qquad (2)$$

where q bisects the angle between the incident and scattered directions which together define the scattering plane. The function $f(q,E)$ gives the amplitude of the radiation coherently scattered by a single atom and is composed of an energy independent part $f_0(q)$ and real and imaginary energy

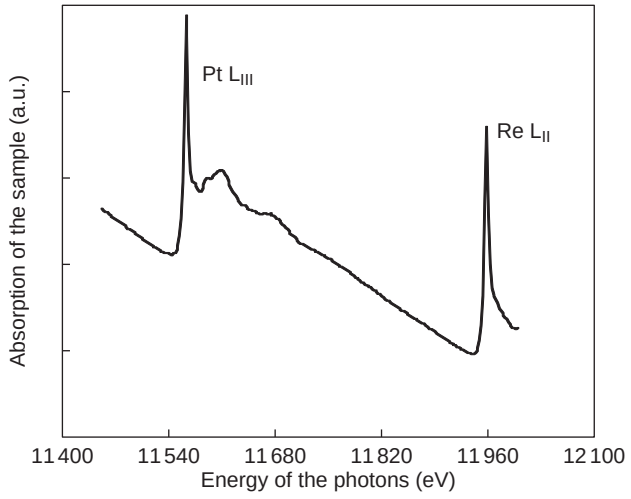

Figure 12

Absorption spectrum collected during an in situ reduction of a 1 weight % Pt-1 weight % Re/Al_2O_3 sample.

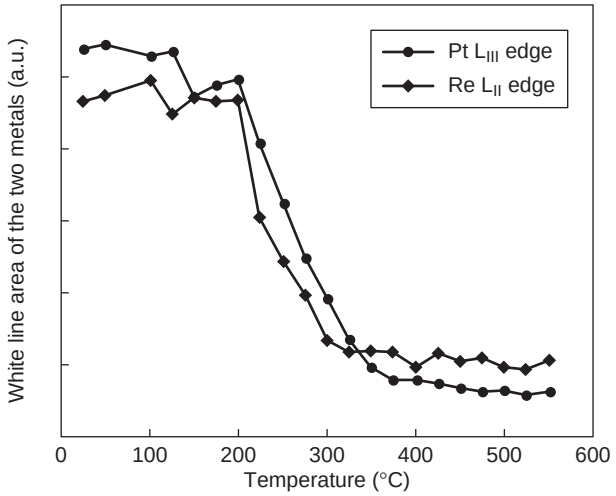

Figure 13

Evolution of the white line intensities of the two metals (platinum and rhenium) during the reduction of a hydrated bimetallic sample.

dependent corrections $f'(E)$ and $f''(E)$. The energy independent part $f_0(q)$ is in fact the usual form factor related to the electron density of the atom:

$$f_0(q) = 4\pi \int_0^\infty \rho(r) \left\{ \frac{\sin(qr)}{qr} \right\} r^3 \, dr \qquad (3)$$

For forward scattering, this parameter tends towards the atomic number Z plus a relativistic correction in the case of medium and heavy elements. The real and imaginary energy dependent corrections, which originate mostly from tightly bound inner electrons, are related through the Kramers-Kronig dispersion relationship. Thus, absorption spectroscopy and anomalous diffraction are intimately related, the imaginary part being linked to the photo-absorption cross section $\sigma(E)$:

$$f'(E) = \frac{2}{\pi} P \int_0^\infty \frac{\varepsilon \, f''(\varepsilon)}{(\varepsilon^2 - E)} \, d\varepsilon$$

and:

$$f''(q,E) = \frac{E \, \sigma(E)}{2hcr_e} \qquad (4)$$

Finally, the diffraction intensity $I(q)$ is given by the Debye scattering equation:

$$I(q) = \sum_i \sum_j f_i(q) \, f_j(q) \left\{ \frac{\sin(qR_{ij})}{qR_{ij}} \right\} \qquad (5)$$

In this equation, $I(q)$ is the angle dependent intensity from coherent scattering, R_{ij} is the distance between atoms i and j with angle dependent atomic scattering factors f_i and f_j. The sums over i and j are over all pairs of atoms.

3.2 The Analysis Procedure

To perform a Fourier analysis of the diffraction diagram, it is convenient to introduce the partial structure factor $S_{mn}(s)$, s being the wave vector, which is related to the pair distribution function by the following relation:

$$S_{nm}(s) = \frac{4\pi}{s} \int_0^\infty (\rho_{nm}(r) - \rho_{n0}) \, r \sin(sr) \, dr \qquad (6)$$

with:

$$s = 4\pi \sin(\theta)/\lambda$$

where $\rho_{mn}(r)$ is the pair distribution function (*i.e.* the density of atoms of type n at a distance r from an atom of type m) and ρ_{n0} is the average atomic density of atoms of type n in the sample. We have then:

$$I(s) = \sum_n \sum_m x_m f_m(s) \, f_n^*(s) \, S_{mn}(s) \qquad (7)$$

where x is the atomic fraction.

3.3 Application to Monometallic Clusters

We now discuss the possibility of using AWAXS to study very small clusters. We consider two families of clusters. Here, calculations have been performed using calculated atomic scattering factors and neglecting thermal disorder and Compton scattering in a first approach. This last approximation is valid since, for the heavy elements considered here, Compton scattering is a small diffuse background which increases slowly when q increases.

As pointed out by Gallezot *et al.* [164], the different diffraction diagrams as well as their FT show Bragg diffraction peaks due to the structure and thus the nature of the network can be directly determined even for very small clusters. In the case of supported materials as it is the case generally, we have to consider the differential intensities, *i.e.* the difference between two diffraction diagrams taken at two energies before the edge.

In the case of monometallic clusters, the differential is similar to the diffraction intensity as shown in Equation (8):

$$\begin{aligned} \Delta I(q) &= \sum_i \sum_j \Delta f_i(q) \, \Delta f_j(q) \left\{ \frac{\sin(qR_{ij})}{qR_{ij}} \right\} \\ &= (\Delta f(q))^2 \sum_i \sum_j \left\{ \frac{\sin(qR_{ij})}{qR_{ij}} \right\} \end{aligned} \qquad (8)$$

Moreover, the splitting between the Bragg peaks is extremely sensitive to the size of the clusters and thus allows a direct measure of the cluster size. This is illustrated in Figure 14 showing a difference diffraction diagram from a study of the reduction of Pd/Al_2O_3. Metal loading here is 0.5% weight so that for classical X-ray diffraction the support contribution is much stronger than the signal from the Pd containing phase. By using differential intensities, the background from the support is eliminated, allowing analysis of the active phase. In Figure 14, the signal from the starting,

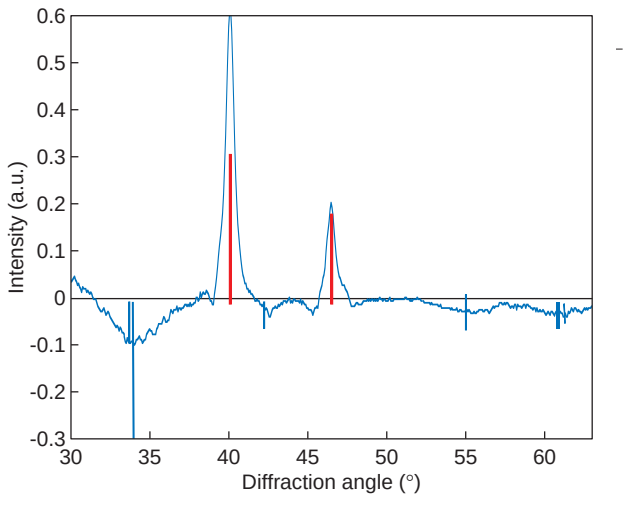

Figure 14

Difference diffraction diagram from a study of the reduction of Pd/Al_2O_3. Reduced phase is positive (c.f. red markers: Pd metal), oxide phase is negative (c.f. blue markers: PdO).

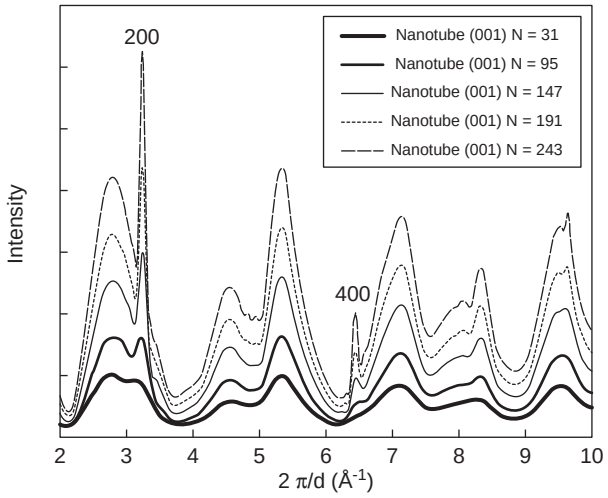

Figure 15

Variation with particle size of the diffraction intensity of a (100) nanotube.

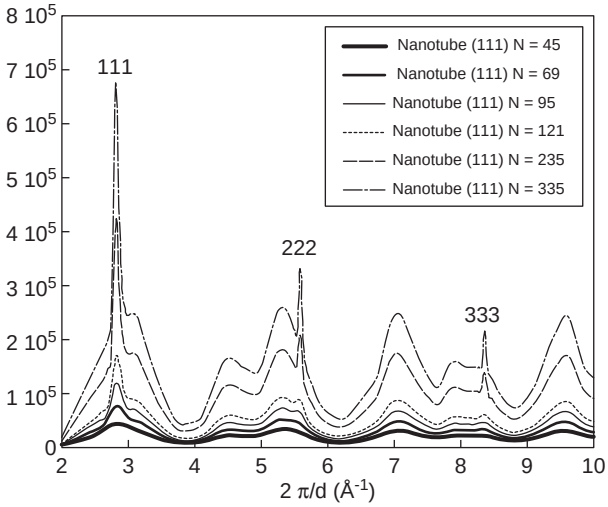

Figure 16

Variation with particle size of the diffraction intensity of a (111) Pt nanotube.

oxide sample has been subtracted from the final, reduced, phase so that the former appears negative (showing dips at the positions corresponding to PdO) whilst the reduced phase is positive (showing peaks at Pd metal positions). The wide oxide peaks, showing that this phase is highly dispersed, give way to sharp metal peaks indicating large particles. The sintering of Pd on reduction suggested by these results was confirmed by MET studies.

Where a distribution of sizes exists, the Debye function analysis method (simulation performed with a linear combination of *ab initio* calculations of diffraction diagrams) developed by Gnutzmann *et al.* [165] can be used and thus information regarding the size distribution is available. On this point, the absorption spectroscopy and the diffraction method can be considered as complementary methods.

Finally, we have considered monometallic clusters which display different morphologies. On Figure 15, we have plotted the diffraction intensity of nanotube clusters for which the growth axis is 100. As we can see, the width of corresponding diffraction intensity is small compared to the other diffraction peaks. An analogous is behaviour is observed if we consider nanotube with 111 growth axis *(Fig. 16)*.

3.4 Applications to Bimetallic Clusters

Here, we consider PtCo bimetallic clusters which exhibit a nanotube morphology. As can be seen in Figure 17, different

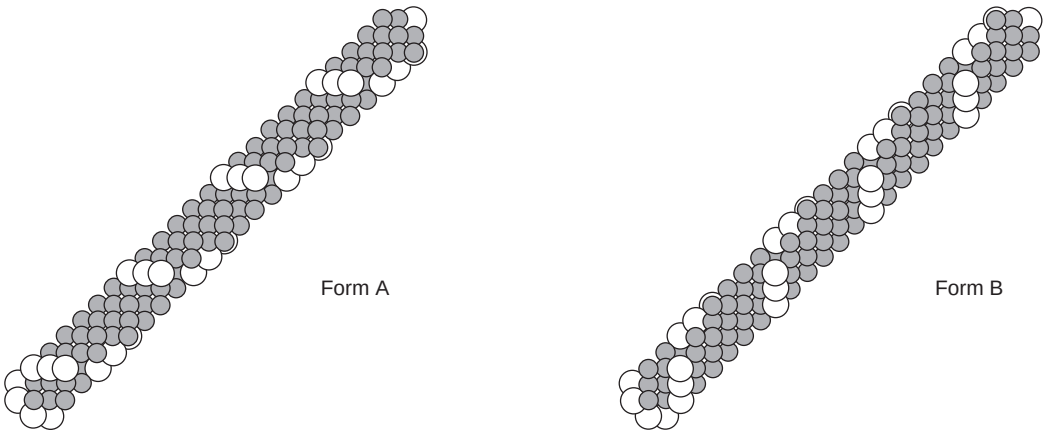

Figure 17

Two enantioforms of a bimetallic cluster.

distributions of the second metal can lead to the construction of two enantiomers. We used tabulated parameters for $f_0(q)$, and Table 1 gives the values of *f'* and *f"* for each element according to Sasaki [166].

It is clear from Figure 18 that the WPSF (weighted sum of partial structure factor) at the platinum and cobalt edges are different when the distribution of the two metals (cobalt and platinum) is not a statistical distribution.

TABLE 1

f' et *f"* for Pt and Pd atoms at different energies

E(eV)	*f'*(Pt)	*f"*(Pt)	*f'*(Co)	*f"*(Co)
7650	– 5.03	7.49	– 4.60	0.48
7700	– 5.05	7.41	– 6.73	0.47
11 450	– 12.25	3.93	0.03	2.03
11 54	– 15.35	3.88	0.04	2.00

4 DISCUSSION

Let's begin by a simple comparison between the Fourier transform of the EXAFS modulations *(Fig. 11)* and the radial distribution function obtained from diffraction data *(Fig. 19)*, the two Fourier transforms being performed on a similar *k* range. The figures show clearly that the diffraction technique is better than absorption spectroscopy for the determination of the local order after the first shell. This is due to the fact that the low *k* range of the absorption spectrum is dominated by multiple scattering processes which lead to a loss of information in the high *r* range.

This advantage has nevertheless to be considered with care. If X-ray scattering factors have similar *k* dependence whatever the atomic number Z (and this is true for wide angle as well as for small angle scattering), it is definitely not the case of the X-ray absorption spectroscopy. Amplitude as well as phase scattering change significantly with atomic number for the latter and thus the chemical sensitivity of the absorption spectroscopy technique is significantly higher. Moreover, as recalled above, information on the electronic state of the absorber atom as well as on the local structure is available through *ab initio* calculations of the "edge" part.

The structural information obtained by AWAXS it is in many cases ambiguous, especially in the case of an overlap of the shells in the same range of distances. This restriction comes from the fact that the technique depends on *n* independent structural factors and it is not possible to decorrelate the $n(n+1)/2$ individual partial structure factors. In fact, there is an evident complementary between the techniques because we need to suppose the nature of the network (given by the AWAXS technique for example) and the morphology (which can be confirmed by AWAXS) to obtain the size of the particle from the different coordination numbers given by absorption spectroscopy.

For bimetallic as well as for multimetallic particles, information regarding the distribution of the two metals inside the cluster can be given by the two techniques and thus a proposed structural model has to be coherent with the different results.

Let us now consider the analysis procedure. One of the major limitations of anomalous diffraction comes from the fact that only a small *k* range of data is available. This is

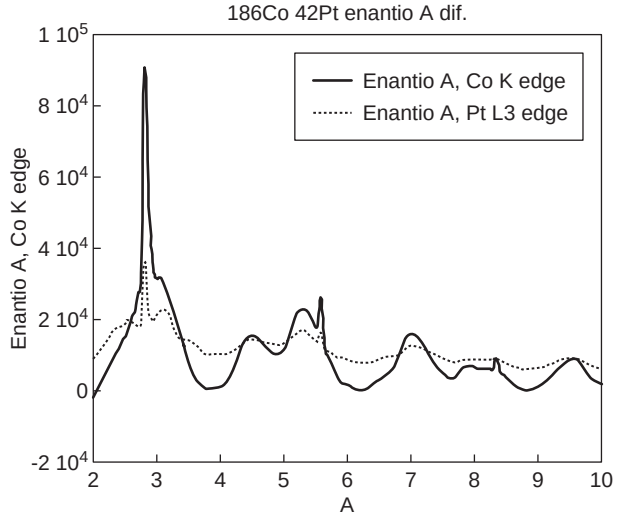

Figure 18

Differences in the WPSF's at the platinum and cobalt edges.

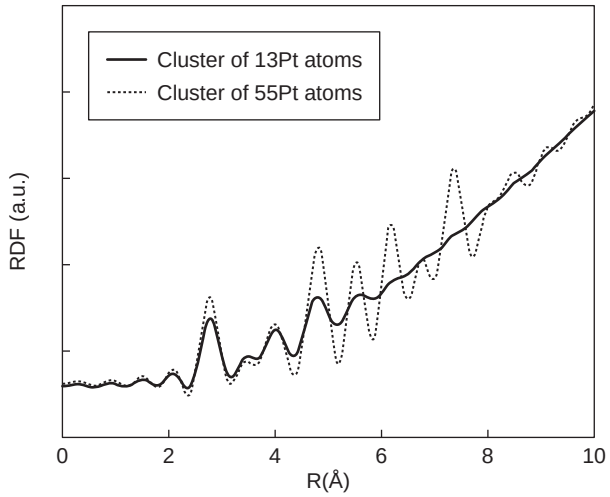

Figure 19

Radial distribution function obtained from diffraction intensity calculated for two clusters containing 13 and 55 platinum atoms.

especially the case for heterogeneous catalysts for which the elements of interest are 3d (and 5d) transition metals which have a K (L) edge around 10 KeV. This implies that the maximum value for k is thus close to 10 $Å^{-1}$ and means that the classical analysis procedure based on the Fourier transform fails at the step of the data normalisation. We have thus to move to *ab initio* calculations using the Debye equation. As shown in this report, we can apply a pseudo Scherrer formula on the differential diagram or compare directly with *ab initio* calculation and this direct analysis procedure allows the size and the structure of the cluster as well as the distribution of the metals inside the particle to be obtained.

From an experimental point of view, it is clear that for low loading supported metallic clusters fewer photons are needed to obtain an absorption spectrum than to build a differential diagram from the diffraction patterns. The anomalous phenomena for wide as well as for small angle scattering is in fact based on a rather weak change in the scattering factor.

CONCLUSION

X-rays techniques related to synchrotron radiation are now widely used for structural characterisation of nanometer scale materials. More precisely, to build an accurate structural model, if laboratory methods constitute the starting point of fundamental research, building a coherent picture of electronic state and particle structure requires information based on these techniques.

From a data analysis point of view, we have shown that for the edge part of the absorption spectra, significant breakthroughs can be obtained based on simulations [133]. For EXAFS, special attention has to be paid to relate the co-ordination number to the size of the cluster or to the distribution of the different elements inside the cluster. Finally, in the case of anomalous diffraction, the Scherrer law can be extended to the differential diagram in the case of monometallic as well as bimetallic systems [73].

TABLE 2

Information obtained by the different techniques

	XANES	EXAFS	AWAXS
Nanometer scale monometallic clusters			
Electronic state	Easy	Difficult	Impossible
Structure	Difficult	Difficult	Easy
Size	Possible	Easy	Possible
Size distribution	Impossible	Difficult	Difficult
Morphology	Impossible	Difficult	Difficult
Nanometer scale bimetallic clusters			
Segregation inside the cluster	Possible	Easy	Difficult

Table 2 provides a synthetic view of the information we can obtain from the different techniques.

It is clear however that only through a correlation with their specific properties, catalytic activities for example, can significant breakthroughs be achieved for various physico-chemical processes.

REFERENCES

1 Somorjai, G.A. (1994) *Principles of Surface Chemistry and Catalysis*. Ed. J. Wiley, New York.

2 Thomas, J.M., Johnson, B.F.G., Raja, R., Sankar, G. and Midgley, P.A. (2002) High-Performance Nanocatalysts for Single-Step Hydrogenations. *Acc. Chem. Res.*, accepted.

3 Somorjai, G.A. and McCrea, K. (2001) Roadmap for Catalysis Science in the 21st Century: A Personal View of Building the Future on Past and Present Accomplishments. *Applied Catalysis A*, **222**, 3.

4 Jacobs, P.W. and Somorjai, G.A. (1998) Conversion of Heterogeneous Catalysis from Art to Science: The Surface Science of Heterogeneous Catalysis. *Journal of Molecular Catalysis A: Chemical*, **131**, 5.

5 Bazin, D. and Guczi, L. (1999) New Opportunities to Understand the Properties on Nanomaterials Through S.R. and Theoretical Calculations. *Recent Res. Dev. Phys. Chem.*, **3**, 387.

6 Boudart, M. (2000) Model Catalysts: Reductionism for Understanding. *Topics in Catalysis*, **13**, 147.

7 Sinfelt, J.H. (2002) Role of Surface Science in Catalysis. *Surface Science*, **500**, 923.

8 Frenkel, A.I., Hills, C.W. and Nuzzo, R.G. (2001) A View from the Inside: Complexity in the Atomic Scale Ordering of Supported Metal Nanoparticles. *J. Phys. Chem. B.*, **105**, 12689.

9 Garin, F. (2001) Mechanism of NOx Decomposition. *Applied Catalysis A: General*, **222**, 183.

10 Sautet, Ph. (2000) Theoretical Chemistry as a Tool for Interpreting Catalysts Selectivities. *Topics in Catalysis*, **13**, 219.

11 Raybaud, P., Schweiger, H., Kresse, G. and Toulhoat, H. (2002) Shape and Edge Sites Modifications of MoS_2 Induced by Working Conditions: a Theoretical Study. *Journal of Catalysis*, **207**, 76.

12 Benco, L., Demuth, T., Hafner, J., Hutschka, F. and Toulhoat, H. (2002) Extraframework Aluminum Species in Zeolites: Ab Initio Molecular Dynamics Simulation of Gmelinite. *Journal of Catalysis*, **209**, 480.

13 Raybaud, P., Digne, M., Iftimie, R., Wellens, W., Toulhoat, H. and Euzen, P. (2001) Morphology and Surface Properties of Boehmite (-AlOOH): A Density Functional Theory Study. *Journal of Catalysis*, **201**, 236.

14 Henry, C. (1998) Surface Studies of Supported Model *Catalysts. Surf. Sci. Rep.*, **31**, 231.

15 Bazin, D., Mottet, C., Treglia, G. and Lynch, J. (2000) New Trends in Heterogeneous Catalysis Processes on Metallic Clusters from Synchrotron Radiation and Theoretical Studies. *Applied Surf. Sci.*, **164**, 140.

16 Bazin, D., Mottet, C. and Treglia, G. (2000) New Opportunities to Understand Heterogeneous Catalysis Processes through Synchrotron Radiation Studies and Theoretical Calculations of Density of States: the Case of

Nanometer Scale Bimetallic Particles. *Applied Catalysis: General A*, **200**, 47.

17 Bazin, D. (2002) Solid State Concepts to Understand Catalysis Using Nanoscale Metallic Particles. *Topics in Catalysis*, **18**, 79.

18 Desjonqueres, M.C. and Spanjaard, D. (1995) *Concepts in Surface Physics*, Ed. Springer.

19 Mottet, C. (1997) Étude par simulation numérique d'agrégats libres mono- et bi-métalliques. *PhD Thesis*, Université Aix-Marseille II.

20 Bertsch, P.M. and Hunter, D.B. (2001) Applications of Synchrotron-Based X-ray Microprobes. *Chem. Rev.*, **101**, 1809.

21 Lynch, J. and Maire, G. (1993) Catalyse hétérogène et SOLEIL, in: *Projet SOLEIL : argumentation scientifique*, Chandesris, D., Morin, P. and Nenner, I. (Eds), Les Éditions de Physique, Les Ulis, 173-178.

22 Lynch, J. (2002) Development of Structural Characterisation Tools for Catalysts. *Oil & Gas Science and Technology*, **57**, 281.

23 Bazin, D., Dexpert, H. and Lynch, J. (1995) *In Situ* XAFS Measurements of Catalysts. Y. Iwasawa, *Xas for Catalyts and Surfaces* (Ed., World Scientific).

24 Bottger, I., Schedel-Niedrig, T., Timpe, O., Gottschall, R., Havecker, M., Ressler, T. and Schlogl, R. (2000) Catalytic Methanol Oxidation Over Copper: Observation of Reaction-Induced Nanoscale Restructuring by Means of *In Situ* Time-Resolved X-Ray Absorption Spectroscopy. *Chemistry - A European Journal*, **6**, 1870.

25 Schneider, S., Bazin, D., Meunier, G., Noirot, R., Capelle, M., Garin, F., Maire, G. and Dexpert, H. (2001) An Exafs Study of Reactant Gases over Nanometer Scale Pt Clusters deposited on γ-Al_2O_3. *Cat. Let.*, **71**, 155.

26 Khodakov, A., Barbouth, N., Oudar, J., Villain, F., Bazin, D., Dexpert, H. and Schulz, P. (1996) Investigation of Dispersion and Localisation of Pt Species in Mazzite Using Exafs. *J. of Phys. Chem.*, **101**, 766.

27 Moonen, J., Lefferts, L., Slot, J., Bazin, D. and Dexpert, H. (1995) The Influence of Polydispersity and Inhomogeneity on Exafs of Bimetallic Catalysts. *Physica B*, **208**, 689.

28 Makishima, H., Tanaka, Y., Kato, Y., Kure, S., Shimada, H., Matsubayashi, N., Nishijima, A. and Nomura, M. (1996) Characterization of Aromatics Saturation Catalysts used in a One-Year Commercial HDS Run. *Catalysis Today*, **29**, 267.

29 Bazin, D., Triconnet, A. and Moureaux, P. (1995) An Exafs Characterisation of the Highly Dispersed Bimetallic PtPd Catalytic System. *NIM B*, **97**, 41.

30 Revel, R., Bazin, D., Dexpert, H. , Elkaim, E. and Seigneurin, A. (2000) An *In Situ* Study Using Awaxs & Xas of the Catalytic System $ZnAl_2O_4$ Supported on Alumina. *J. Phys. Chem. B*, **104**, 9828.

31 Bourges, P., Garin, F., Maire, G., Szabo, G., Laborde, M., Loutaty, R. and Bazin, D. (1996) Étude *in situ* par analyse Exafs d'un catalyseur de reformage $PtSn/Al_2O_3$-Cl. *J. de Physique*, **C4-6**, 947.

32 Carriat, J.Y., Che, M., Kermarec, M., Verdaguer, M. and Michalowicz, A. (1998) Control of Dispersion of Ni Ions via Chelate Ligands in the Preparation of Ni/SiO_2 Materials. A XAFS Study. *J. of the American Chemical Society*, **120**, 2059.

33 Chester, A.W., Absil, R.P.A., Kennedy, G.J., Lagarde, P. and Flank, A.M. (1999) X-Ray Absorption Spectroscopy of Transition Aluminas. *J. Synchrotron Rad.*, **6**, 448.

34 McBreen, J. and Sansone, M. (1994) *In Situ* X-Ray Absorption Spectroscopic Study of Adsorbed Pb on Carbon-Supported Pt. *Journal of Electroanalytical Chemistry*, **373**, 227.

35 Bazin, D. and Guczi, L. (2001) Soft X-Ray Absorption Spectroscopy and Heterogeneous Catalysis. *Applied Catalysis General A*, **213**, 147.

36 Bazin, D., Guczi, L. and Lynch, J. (2002) AWAXS in Heterogeneous Catalysis. *Applied Catalysis General A*, **87**, 226.

37 Hodeau, J.L., Favre-Nicolin, V., Bos, S., Renevier, H., Lorenzo, E. and Berar, J.F. (2001) Resonant Diffraction. *Chem. Rev.*, **101**, 1843.

38 Védrine, J.C. (2000) Industrial Features. *Catalysis Today*, **56**, 333.

39 Lynch, J. (1994) Characterisation of Industrial Catalysts by EXAFS. *Journal de Physique III*, **4-C9**, 253.

40 Plazenet, G., Payen, E., Lynch, J. and Rebours, B. (2002) Study by EXAFS, Raman, and NMR Spectroscopies of the Genesis of Oxidic Precursors of Zeolite-Supported HDS Catalysts. *J. Phys. Chem. B.*, **106**, 7013.

41 Marcilly, C.R. (2000) Where and How Shape Selectivity of Molecular Sieves Operates in Refining and Petrochemistry Catalytic Processes. *Topics in Catalysis*, **13**, 357.

42 Barbier Jr., J., Oliviero, L., Renard, B. and Duprez, D. (2002) Catalytic Wet Air Oxidation of Ammonia over M/CeO_2 Catalysts in the Treatment of Nitrogen-Containing Pollutants. *Catalysis Today*, **75**, 29.

43 Del Angel, P., Dominguez, J.M., Del Angel, G., Montoya, J.A., Lamy-Pitara, E., Labruquere, S. and Barbier, J. (2000) Aggregation State of Pt-Au/C Bimetallic Catalysts Prepared by Surface Redox Reactions. *Langmuir*, **16**, 7210.

44 Demirci, Ü.B. and Garin, F. (2002) Kinetic Study of *n*-heptane Conversion on Sulfated Zirconia-Supported Platinum Catalyst: The Metal-Proton Adduct is the Active Site. *Journal of Molecular Catalysis A: Chemical*, **188**, 233.

45 Lemaux, S., Bensaddik, A., van der Eerden, A.M.J., Bitter, J.H. and Koningsberger, D.C. (2001) Understanding of Enhanced Oxygen Storage Capacity in $Ce_{0.5}Zr_{0.5}O_2$: the Presence of an Anharmonic Pair Distribution Function in the Zr-O_2 Subshell as Analyzed by XAFS Spectroscopy. *J. Phys. Chem. B.*, **105**, 4810.

46 Dauscher, A., Touroude, R., Maire, G., Kizling, J., Boutonnet-Kizling, M. (1993) Influence of the Preparation Mode on Metal-Support Interactions in Pt/TiO_2 Catalysts. *Journal of Catalysis*, **143**, 155.

47 Marecot, P., Fakche, A., Pirault, L., Geron, C., Mabilon, G., Prigent, M. and Barbier, J. (1994) Effect of the Preparation Procedure on the Properties of Three-Way Automotive PtRh/Alumina-Ceria Catalysts. *Applied Catalysis B: Environmental*, **5**, 43.

48 Bigey, C., Hilaire, L. and Maire, G. (2001) WO_3-CeO_2 and Pd/WO_3-CeO_2 as Potential Catalysts for Reforming Applications. I. Physicochemical Characterization Study. *Journal of Catalysis*, **198**, 208.

49 Didillon, B., Bachir, R., Marecot, P. and Barbier, J. (1997) Isoprene Hydrogenation on Supported Pd-Fe Catalysts. Influence of the Catalyst Preparation Procedure. *Applied Catalysis A: General*, **164**, 313.

50 Kerkeni, S., Lamy-Pitara, E. and Barbier, J. (2002) Copper-Platinum Catalysts Prepared and Characterized by Electro-Chemical Methods for the Reduction of Nitrate and Nitrite. *Catalysis Today*, **75**, 35.

51 Epron, F., Gauthard, F. and Barbier, J. (2002) Influence of Oxidizing and Reducing Treatments on the Metal-Metal Inter-

actions and on the Activity for Nitrate Reduction of a Pt-Cu Bimetallic Catalyst. *Applied Catalysis A: General*, **237**, 253.

52 Garin, F., Girard, P., Ringler, S., Maire, G. and Davias, N. (1999) Mechanistic Studies of NO(x) Reduction Reactions under Oxidative Atmosphere on Alumina Supported 1 wt% Pt and 1 wt% Pt-0.5 wt% Zn Catalysts (Part I). *Applied Catalysis B: Environmental*, **20**, 205.

53 Védrine, J.C., Coudurier, G., Ouqour, A., Pries de Oliveira, P.G. and Volta, J.C. (1996) Niobium Oxide Based Materials as Catalysts for Acidic and Partial Oxidation Type Reactions. *Catalysis Today*, **28**, 3.

54 Oliviero, L., Barbier Jr., J., Duprez, D., Wahyu, H., Ponton, J.W., Metcalfe, I.S. and Mantzavinos, D. (2001) Wet Air Oxidation of Aqueous Solutions of Maleic Acid over Ru/CeO_2 Catalysts. *Applied Catalysis B: Environmental*, **35**, 1.

55 Delage, M., Didillon, B., Huiban, Y., Lynch, J. and Uzio, D. (2000) Highly Dispersed Pd Based Catalysts for Selective Hydrogenation Reactions. *Studies in Surface Science and Catalysis*, **130**, 1019.

56 Euzen, P., Le Gal, J.H., Rebours, B. and Martin, G. (1999) Deactivation of Palladium Catalyst in Catalytic Combustion of Methane. *Catalysis Today*, **47**, 19.

57 Merlen, E., Beccat, P., Bertolini, J.C., Delichère, P., Zanier, N. and Didillon, B. (1996) Characterization of Bimetallic Pt-Sn/Al_2O_3 Catalysts: Relationship between Particle Size and Structure. *Journal of Catalysis*, **159**, 178.

58 Katrib, A., Mey, D. and Maire, G. (2001) Molybdenum and Tungsten Dioxides, XO_2 (X = Mo,W), as Reforming Catalysts for Hydrocarbon Compounds. *Catalysis Today*, **65**, 179.

59 Marécot, P., Mahoungou, J.R. and Barbier, J. (1993) Benzene Hydrogenation on Platinum and Iridium Catalysts. Variation of the Toxicity of Sulfur with the Nature of the Support. *Applied Catalysis A: General*, **101**, 143.

60 Locatelli, F., Didillon, B., Uzio, D., Niccolai, G., Candy, J.P. and Basset, J.M. (2000) Preparation and Characterization of Small Silica-Supported Iridium Particles from Iridium Trisacetylacetonate Precursor. *Journal of Catalysis*, **193**, 154.

61 Bensaddik, A., Dexpert, H., Bazin, D., Villain, F., Didillon, B. and Lynch, J. (1995) *In Situ* Study by XAS of the Sulfuration of the Pt and $PtRe/Al_2O_3$ Systems. *Physica B*, **208**, 677.

62 Shelimov, B., Lambert, J.F., Che, M. and Didillon, B. (1999) Initial Steps of the Alumina-Supported Platinum Catalyst Preparation: a Molecular Study by 195Pt NMR, UV¯Visible, EXAFS, and Raman Spectroscopy. *Journal of Catalysis*, **185**, 462.

63 Espinosa, G., Del Angel, G., Barbier, J., Bosch, P., Lara, V. and Acosta, D. (2000) Catalytic Behavior and Active Sites Structure of $PtAu/Al_2O_3$ Bimetallic Catalysts Prepared by Surface Redox Reactions. *Journal of Molecular Catalysis A: Chemical*, **164**, 253.

64 Leyrit, P., Cseri, T., Marchal, N., Lynch, J. and Kasztelan, S. (2001) Aromatic Reduction Properties of Molybdenum Sulfide Clusters in HY Zeolite. *Catalysis Today*, **65**, 249.

65 Payen, E., Plazenet, G. and Lynch J. (2002) Cobalt-Molybdenum Interaction in Oxidic Precursors of Zeolite-Supported HDS Catalysts. *Physical Chemistry Chemical Physics*, **4**, 3924.

66 Plazenet, G., Cristol, S., Paul, J.F., Payen, E. and Lynch, J. (2001) Sulfur Coverage and Structural Disorder in Alumina-Supported MoS_2 Crystallites: an *In Situ* EXAFS Study. *Physical Chemistry Chemical Physics*, **3**, 246.

67 Afanasiev, P., Bezverkhyy, I., Geantet, C. and Lacroix, M. (2001) Highly Active (Co) MoS_2/Al_2O_3 Hydrodesulfurization Catalysts Prepared in Aqueous Solution. *Journal of Catalysis*, **204**, 495.

68 Gonzalez, M.G., Ponzi, E.N., Ferretti, O.A., Quincoces, C.E., Marecot, P. and Barbier, J. (2000) Studies on H_2S Adsorption and Carbon Deposition over $Mo\text{-}Ni/Al_2O_3$ Catalysts. *Adsorption Science and Technology*, **18**, 541.

69 Bezverkhyy, I., Afanasiev, P., Geantet, C. and Lacroix, M. (2001) Highly Active $(Co)MoS_2/Al_2O_3$ Hydrodesulfurization Catalysts Prepared in Aqueous Solution. *Journal of Catalysis*, **204**, 495.

70 Gaborit, V., Allali, N., Geantet, C., Breysse, M., Vrinat, M. and Danot, M. (2000) Niobium Sulfide as a Dopant for Hydrotreating NiMo Catalysts. *Catalysis Today*, **57**, 267.

71 Enache, D.I., Rebours, B., Roy-Auberger, M. and Revel, R. (2002) *In situ* XRD Study of the Influence of Thermal Treatment on the Characteristics and the Catalytic Properties of Cobalt-Based Fischer-Tropsch Catalysts. *Journal of Catalysis*, **205**, 346.

72 Khodakov, A., Ducreux, O., Lynch, J., Rebours, B. and Chaumette, P. (1999) Structural Modification of Cobalt Catalysts: Effect of Wetting Studied by X-Ray and Infrared Techniques. *Oil and Gas Science and Technology*, **54**, 525.

73 Bazin, D., Sayers, D. and Rehr, J. (1997) Comparison between Xas, Awaxs, Asaxs & Dafs Applied to Nanometer Scale Metallic Clusters. *J. Phys. Chem.*, **101**, 11040.

74 Bazin, D. and Sayers, D. (1993) Comparison between Xas & Awaxs Applied to Nanometer Scale Supported Bimetallic Clusters. *Jpn J. Appl. Phys.*, **32-2**, 249.

75 Wong, J., George, G.N., Pickering, I.J., Rek, Z.U., Rowen, M., Tanaka, T., Via, G.H., DeVries B., Vaughan, D.E.W., and Brown, G.E., Jr. (1994) New Opportunities in XAFS Investigation in the 1-2 keV Region. *Solid State Communications*, **92**, 559.

76 de Groot, F. (2001) High-Resolution X-ray Emission and X-ray Absorption Spectroscopy. *Chem. Rev.*, **101**, 1779.

77 Denbeaux, G., Andersona, E., Chaoa, W., Eimüller, T., Johnson, L., Köhler, M., Larabell, C.M., Legrosa, M., Fischer, P., Pearson, A., Schütz, G., Yager, D. and Attwood, D. (2001) Soft X-Ray Microscopy to 25 nm with Applications to Biology and Magnetic Materials. *NIM A*, **467-468**, 841.

78 Schedel-Niedrig, Th., Hävecker, M., Knop-Gericke, A., Reinke, P., Schlöl, R. and Lux-Steiner, M.Ch. (2001) *In situ* X-Ray Absorption Spectroscopy in the Soft Energy Range: Novel Prospects for the Chemical Characterization of Solid State Surfaces at High Pressure and High Temperature. *Materials Research Society Symposium - Proceedings*, **678**, EE8.3.

79 Hävecker, M., Knop-Gericke, A. and Schedel-Niedrig, Th. (1999) High-Pressure Soft X-Ray Absorption Spectroscopy: Application of a New *In Situ* Spectroscopic Method in Catalysis Research. *Applied Surface Science*, **142**, 438.

80 Srivastava, P. and Baberschke, K. (2000) New Opportunities in Soft X-Ray Absorption to Characterise the Adsorbate Bonding. *Topics in Catalysis*, **10**, 199.

81 Jun, K., Yoshinobu, M., Tetsuro, S., Makoto, S., Tohru, H., Yoshihisa, H., Yoichi, I. Akiko, F., Masami, F., Masamitsu, W., Kuniko, M., Shik, S. and Yohichi, G. (2000) High Resolution Soft X-Ray Absorption Spectroscopy for the Chemical State Analysis of Mn. *Spectrochimica Acta - Part B Atomic Spectroscopy*, **55**, 1385.

82 Havecker, M., Knop-Gericke, A., Schedel-Niedrig, T. and Schlogl, R. (1998) High-Pressure Soft X-Ray Absorption Spectroscopy: a Contribution to Overcoming the "Pressure Gap" in the Study of Heterogeneous Catalytic Processes. *Angewandte Chemie - International Edition*, **37**, 1939.

83 Chen, J.G. (1997) NEXAFS Investigations of Transition Metal Oxides, Nitrides, Carbides, Sulfides and Other Interstitial Compounds. *Surf. Sci. Report*, **30**, 1.

84 Knop-Gericke, A., Havecker, M., Schedel-Niedrig, Th. and Schlog, R. (2000) *Topics in Catalysis*, **10**, 187.

85 Srivastava, P., Baberschke, K (2000) New Opportunities in Soft X-Ray Absorption to Characterise the Adsorbate Bonding. *Topics in Catalysis*, **10**, 199.

86 Shimada, H. (2000) Characterization of Coke Deposited on Catalysts by Carbon K-Edge near Edge X-Ray Absorption Fine Structure (NEXAFS) Spectroscopy. *Topics in Catalysis*, **10**, 265.

87 Mayer, R.W. (2001) Investigation of Ammonia Oxidation over Copper with *In Situ* NEXAFS in the Soft X-Ray Range: Influence of Pressure on the Catalyst Performance. *Catalysis Letters*, **74**, 119.

88 Van Bokhoven, J.A., Sambe, H., Ramaker, D.E. and Koningsberger, D.C. (1999) Al K-Edge Near-Edge X-Ray Absorption Fine Structure (NEXAFS) Study on the Coordination Structure of Aluminum in Minerals and Y Zeolites. *J. Phys. Chem. B.*, **103**, 7557.

89 Van Bokhoven, J.A., Koningsberger, D.C., Kunkeler, P. and van Bekkum, H. (2002) Influence of Steam Activation on Pore Structure and Acidity of Zeolite Beta: An Al K Edge XANES Study of Aluminum Coordination. *J. of Catalysis*, **211**, 540.

90 Okajima, T., Teramoto, K., Mitsumoto, R., Oji, H., Yamamoto, Y., Mori, I., Ishii, H., Ouchi, Y. and Seki, K. (1998) *J. Phys. Chem. A.*, **102**, 7093.

91 Parent, Ph., Laffon, C., Tourillon, G. and Cassuto, A. (1995) *J. Phys. Chem.*, **99**, 5058.

92 Terada, S., Yokoyama, T., Sakano, M., Imanishi, A., Kitajima, Y., Kiguchi, M., Okamoto, Y., Ohta, T. (1998) Thiophene Adsorption on Pd(111) and Pd(100) Surfaces Studied by Total-Reflection S K-Edge X-Ray Absorption Fine-Structure Spectroscopy. *Surface Science*, **414**, 107.

93 Bazin, D., Kovacs, I., Guczi, L., Parent, P., Laffon, C., De Groot, F., Ducreux, O., Lynch, J. (1999) Following the Reduction under H_2 of Supported Co Catalysts Through the L Absorption Edges. *J. Syn. Rad. News*, **6**, 430.

94 Abbate, M., Pen, H., Czyyk, M.T., de Groot, F.M.F., Fuggle, J.C., Ma, Y.J., Chen, C.T., Sette, F., Fujimori, A., Ueda, Y. and Kosuge, K. (1993) Soft X-Ray Absorption Spectroscopy of Vanadium Oxides. *J. of Electron Spectroscopy and Related Phenomena*, **62**, 185.

95 Amemiya, K., Kondoh, H., Yokoyama, T. and Ohta, T. (2002) A Soft X-Ray Beamline for Surface Chemistry at the Photon Factory. *J. of Electron Spectroscopy and Related Phenomena*, **124**, 151.

96 Pompa, M., Flank, A.M., Lagarde, P., Rife, J., Stekhin, I., Nakazawa, M., Ogasawara, H. and Kotani, A. (1997) Experimental and Theoretical Comparison between Absorption, Total Electron Yield and Fluorescence Spectra of the Thumllium M5 edge. *J. de Phys. IV*, **C2-III**, 159.

97 Cabaret, D., Sainctavit, Ph., Ildefonse, Ph. and Flank, A.M. (1997) Determination of Mg Site Geometry in Pyroxenes by Full Multiple Scattering Calculations. *J. de Phys. IV*, **C2-III**, 157.

98 Parent, Ph., Laffon, C., Tourillon, G. and Cassuto, A. (1995) Adsorption of Acrylonitrile on Pt(111) and Au(111) at 95 K in the Monolayer and Multilayer Ranges Studied by NEXAFS, UPS, and FT-IR. *J. Phys. Chem.*, **99**, 5058-5066.

99 Revel, R., Parent, P., Laffon, C. and Bazin, D. (2001) NO adsorption on Zn/Al_2O_3 Powder: Nexafs Study at Nitrogen K edge. *Cat. Let.*, **74**, 189.

100 Rompel, A, Cinco, R.M., Robblee, J.H., Latimer, M.J., McFarlane, K.L., Huang, J., Walters, M.A. and Yachandra, V.K. (2001) S K- and Mo L-Edge X-Ray Absorption Spectroscopy to Determine Metal-Ligand Charge Distribution in Molybdenum-Sulfur Compounds. *J. of Synchrotron Radiation*, **8**, 1006.

101 Izumi, Y., Glaser, T., Rose, K., McMaster, J., Basu, P., Enemark, J.H., Hedman, B., Hodgson, K.O. and Solomon, E.I. (1999) Ligand K-Edge and Metal L-Edge X-Ray Absorption Spectroscopy and Density Functional Calculations of Oxomolybdenum Complexes with Thiolate and Related Ligands: Implications for Sulfite Oxidase. *J. of the American Chemical Society*, **121**, 10035.

102 Glaser, T., Rose, K., Shadle, S.E., Hedman, B., Hodgson, K. O. and Solomon, E.I., (2001) S K-Edge X-Ray Absorption Studies of Tetranuclear Iron-Sulfur Clusters: M-Sulfide Bonding and its Contribution to Electron Delocalization. *J. of the American Chemical Society*, **123**, 442.

103 Farrell, S.P. and Fleet, M.E. (2001) Sulfur K-Edge XANES Study of Local Electronic Structure in Ternary Monosulfide Solid Solution (Fe, Co, Ni)0.923S. *Physics and Chemistry of Minerals*, **28**, 17.

104 Waldo, G.S., Carlson, R.M.K., Moldowan, J.M., Peters, K.E. and Penner-Hahn J.E. (1991) *Geochim. et Cosmochim. Acta*, **55**, 801.

105 Lynch, J., Everlien, G., Leblond, C., Bazin, D. (1999) Evolution of Sulphur During Pyrolysis of Petroleum Kerogens, *J. of Synchrotron Radiation*, **6**, 661.

106 Guczi, L., Schay, G., Stefler, G. and Mizukami, F. (1999) Bimetallic Catalysis: CO hydrogenation over PdCo Catalysts Prepared by Sol/Gel Method. *J. Mol. Catal. A.*, **141**, 177.

107 Guczi, L., Borkó, L., Koppány, Zs. and Mizukami, F. (1998) *Catal. Lett.*, **54**, 33.

108 Guczi, L., Sundararajan, R., Koppány, Zs., Zsoldos, Z., Schay, Z., Mizukami, F. and Niwa, S. (1997) Structure and Characterization of Supported RuCo Bimetallic Catalysts. *J. Catal.*, **167**, 482.

109 Udayan D. (2002) Studies on Some Advanced Materials and Use of the Singapore Synchrotron Light Source. *NIM B*, in press.

110 Clausen, B.S. (1998) Combined (Q)EXAFS/XRD: Technique and Applications. *Catalysis Today*, **39**, 293.

111 Meneau, F., Sankar, G., Morgante, N., Cristol, S., Catlow, C.R.A., Thomas, J.M. and Greaves, G.N. (2002) Characterization of Zinc Oxide Nanoparticles Encapsulated into Zeolite-Y: An *In Situ* Combined X-Ray Diffraction, XAFS, and SAXS Study. *NIM B*, in press.

112 Thomas, J.M. and Sankar, G (2001) The Role of Synchrotron-Based Studies in the Elucidation and Design of Active Sites in Titanium-Silica Epoxidation Catalysts. *Accounts of Chemical Research*, **34**, 571.

113 Grunwaldt, J.D., Molenbroek, A.M., Topsøe, N.Y., Topsøe, H. and Clausen, B.S. (2000) *In Situ* Investigations of Structural Changes in Cu/ZnO Catalysts. *Journal of Catalysis*, 194, 452.

114 Dent, A.J., Oversluizen, M., Greaves, G.N., Roberts, M.A., Sankar, G., Catlow, C.R. and Thomas, J.M. (1995) A Furnace Design for Use in Combined X-Ray Absorption and Diffraction up to a Temperature of 1200°C: Study of Cordierite Ceramic Formation Using Fluorescence QEXAFS/ XRD. *Physica B: Condensed Matter*, **208-209**, 253.

115 Epple, M., Sankar, G. and Thomas, J.M. (1997) Solid-State Polymerization Reaction by Combined *In-Situ* X-ray

Diffraction and X-ray Absorption Spectroscopy (XRD-EXAFS). *Chem. Mater.*, **9**, 3127.

116 Evans, J. and Newton, M.A (2002) Towards a Structure-Activity Relationship for Oxide Supported Metals. *J. of Molecular Catalysis A: Chemical*, **182**, 351

117 Cimini, F. and Prins, R. (1997) QEXAFS Investigation of the Particle Growth of PtRh Clusters Supported on NaY. *J. Phys. Chem. B.*, **101**, 5277.

118 Sun, M., Bürgi, T., Cattaneo, R., van Langeveld, D. and Prins R. (2001) TPS, XPS, QEXAFS, and XANES Investigation of the Sulfidation of NiW/Al_2O_3-F Catalysts. *J. of Catalysis*, **201**, 258.

119 Sun, M., Bürgi, T., Cattaneo, R. and Prins, R. (2001) TPS, XPS, and QEXAFS Investigation of the Sulfidation Behavior of Tungsten on Fluorine-Promoted Alumina. *J. of Catalysis*, **197**, 172.

120 Lamberti, C., Prestipino, C., Bonino, F., Capello, L., Bordiga, S., Spoto, G., Zecchina, A., Moreno, S.D., Cremaschi, B., Garilli, M., Marsella, A., Carmello, D., Vidotto, S. and Leofanti, G. (2002) The Chemistry of the Oxychlorination Catalyst: an *In Situ*, Time-Resolved XANES Study. *Angewandte Chemie - International Edition*, **41**, 2341.

121 Nghiem, P., Tordeux, M.A. and Level, M.P. (2002) Study on Coupling and Coupling Correction for the SOLEIL Ring. *NIM A*, **480**, 339.

122 Ciret, J.C., Congretel, G., Evesque, C. and Gros, P. (2000) Eddy Current Septum Magnet Prototype for SOLEIL Light Source Project. IEEE *Transactions on Applied Superconductivity*, **10**, 244.

123 http://www.soleil.u-psud.fr

124 Gailhanou, M., Dubuisson, J.M., Ribbens, M., Roussier, L., Bétaille, D., Créoff, C., Lemonnier, M., Denoyer, J., Bouillot, C., Jucha, A., Lena, A., Idir, M., Bessière, M., Thiaudière, D., Hennet, L., Landron, C., Coutures, J.P. (2001) H10: a Materials and High Temperature Beamline at LURE/DCI. *NIM A*, **467-468**, 745.

125 Adora, S., Soldo-Olivier, Y., Faure, R., Durand, R., Dartyge, E., Baudelet, F. (2001) Electrochemical Preparation of Platinum Nanocrystallites on Activated Carbon Studied by X-ray Absorption Spectroscopy. *J. Phys. Chem. B.*, **105**, 10489.

126 Lytle, F.W., Wei, P.S.P., Greegor, R.B., Via, G.H. and Sinfelt, J.H. (1979) Effect of Chemical Environment on Magnitude of X-Ray Absorption Resonnance at L_{III} Edges. Studies on Metallic Elements, Compounds and Catalysts. *J. Chem. Phys.*, **70**, 4849.

127 Mansour, A.N., Cook, J.W. and Sayers, D.E. (1984) Quantitative Technique for the Determination of the Number of Unoccupied d-Electron States in a Platinum Catalysts using the LII,III X-Ray Absorption Edge Spectra. *J. Phys. Chem.*, **88**, 2330.

128 Bazin, D., Maire, F., Schneider, S., Meunier, G., Maire, G. (1997) A Detailed Study of the Metallic Function of Bimetallic PtRh Post Combustion Catalyst by Xas, Met: Correlation with their Catalytic Activity. *J. de Phys. IV*, **C2**, 841.

129 Koningsberger, D.C. and Mojet, L. (2000) Role an Contributions of Xafs Spectroscopy in Catalysis.

130 Bazin, D., Sayers, D.E., Rehr, J.J. and Mottet, C. (1997) Numerical Simulation of the Pt L_{III} Edge White Line Relative to Nanometer Scale Clusters. *J. of Phys. Chem.*, **101**, 5332.

131 Fernandez-Garcia, M., Marquez Alvarez, C. and Haller, G.L. (1995) XANES-TPR Study of Cu-Pd Bimetallic Catalysts: Application of Factor Analysis. *J. Phys. Chem.*, **99**, 12565.

132 Fernandez-Garcia, M., Martinez-Arias, A., Rodriguez-Ramos, I., Ferreira-Aparicio, P. and Guerrero-Ruiz, A. (1999) Genesis of Surface and Bulk Phases in RhCo Catalysts. *Langmuir*, **15**, 5295.

133 Bazin, D. and Rehr, J.J. Limits and Advantages of X-Ray Absorption Near Edge Structure for Nanometer Scale Metallic Clusters, accepted in *J. Phys. Chem.*

134 Bazin, D., Bensaddik, A., Briois, V. and Saintavict, Ph. (1996) M. S. Calculation of Xas and XRD Calculations: Application to Nanometer Scale Cu Metallic Particle. *J. de Physique*, **C4**, 481.

135 Stern, E.A. (1975) Extended X-Ray Absorption Fine Structure Techniquez. II - Experimental Practice and Selected Results. *Phys. Rev B*, **11**, 4825.

136 Szaloki, I., Torok, S.B., Injuk, J. and Van Grieken, R.E. (2002) X-Ray Spectrometry. *Anal. Chem.*, **74**, 2895.

137 Michalowicz, A. and Vlaic, G. (1998) Multiple Solutions in Data Fitting: a Trap in EXAFS Structural Analysis and Some Ideas to Avoid It. *J. Synch. Rad.*, **5**, 1317.

138 Koningsberger, D.C., Mojet, B.L., van Dorssen, G.E. and Ramaker, D.E (2000) XAFS Spectroscopy; Fundamental Principles and Data Analysis. *Topics in Catalysis*, **10**, 143.

139 Bazin, D., Dexpert, H., Lagarde, P. and Bournonville, J.P. (1988) Xas Studies of Bimetallic Pt-Re(Rh)/Al_2O_3 Catalysts in the First Stages of Preparation. *J. of Cat.*, **110**, 209.

140 Douidah, A., Marécot, P., Szabo, S. and Barbier, J. (2002) Evaluation of the Metal-Support Interactions - Case of Platinum-Supported Catalysts: Effect of the Support Nature and the Metallic Dispersion. *Applied Catalysis A: General*, **225**, 21.

141 Koningsberger, D.C., Oudenhuijzen, M.K., Tappel, B., Van Bokhoven, Kooyman, P.J. (2002) Understanding the Influence of the Pretreatment Procedure on Platinum Particle Size and Particle-Size Distribution for SiO_2 Impregnated with $[Pt(NH_3)_4](NO_3)_2$: a Combination of HRTEM, mass Spectrometry, and quick EXAFS. *J. of Catalysis*, **205**,135.

142 Koningsberger, D.C., De Graaf, J., Van Dillen, A.J. and De Jong, K.P. (2001) Preparation of Highly Dispersed Pt Particles in Zeolite Y with a Narrow Particle Size Distribution: Characterization by Hydrogen chemisorption, TEM, EXAFS Spectroscopy, and Particle Modeling. *Journal of Catalysis*, **203**, 307.

143 Vaarkamp, M., Miller, J.T., Modica, F.S. and Koningsberger, D.C. (1996) On the Relation between Particle Morphology, Structure of the Metal-Support Interface, and Catalytic Properties of Pt/-Al_2O_3. *J. of Catalysis*, **163**, 294.

144 Fung, A.S., Kelley, M.J., Koningsberger, D.C. and Gates, B.C. (1997) γ-Al_2O_3-Supported Re-Pt Cluster Catalyst Prepared from $[Re_2Pt(CO)_{12}]$: Characterization by EXAFS and Catalysis of Methylcyclohexane Dehydrogenation. *J. Am. Chem. Soc.*, **119**, 5877.

145 Espinosa, G., Del Angel, G., Barbier, J., Bosch, P., Lara, V. and Acosta, D. (2000) Catalytic Behavior and Active Sites Structure of PtAu/Al_2O_3 bimetallic catalysts prepared by surface redox reactions. *Journal of Molecular Catalysis A: Chemical*, **164**, 253.

146 Bazin, D., Dexpert, H., Lynch, J. and Bournonville, J.P. (1999) Xas of Electronic State Correlations During the Reduction of the Bimetallic PtRe/Al_2O_3. *System. J. of Syn. Rad.*, **6**, 465.

147 Stachs, O., Petkov, V., Himmel, B. and Gerber, T. (1999) Secondary Graphite Crystal Spectrometer for Anomalous X-Ray Diffraction Experiments. *NIM A*, **434**, 473.

148 Ramos, S., Neilson, G.W., Barnes, A.C. and Mazuelas, A. (2001) An Anomalous X-Ray Diffraction Study of Yttrium (III) Hydration. *J. Phys. Chem. B.*, **105**, 2694.

149 Serimaa, R., Etelaniemi, V., Laitalainen, T., Bienenstock, A., Vahvaselka, S. and Paakkari, T. (1997) Structure of Amorphous Platinum Uridine Green Sulfate by AWAXS and EXAFS. *Inorg. Chem.*, **36**, 5574.

150 Sayers, D.E., Renevier, H., Hodeau, J.L., Berar, J.F., Tonnerre, J.M., Raoux, D., Chester, A., Bazin, D. and Bouldin, C. (1997) On the Way to Understanding Platinum in a Pt-Zeolite Catalyst. *ESRF NewsLetter*, **27**.

151 Bazin, D., Revel, R., Dexpert, H., Elkaim, E., Lauriat, J., Garin, F., Maire, F. and Guczi, L. (1998) Aspects complémentaires entre Xas et Awaxs dans le cas d'entités de taille nanométrique supportés sur un oxide léger : agrégats métalliques et spinelle. *J. de Phys.*, **IV/8**, 263.

152 Balerna, A., Liotta, L., Longo, A., Martorana, A., Meneghini, C., Mobilio, S. and Pipitone, G. (1999) Structural Characterization of Pumice-Supported Silver-Palladium Metal Clusters by Means of XAFS and AWAXS. *Eur. Phys. J. D*, **7**, 89.

153 Samant, M.G., Bergeret, G., Meitzner, G. and Boudart, M. (1988) Anomalous Wide Angle X-Ray Scattering and X-Ray Absorption Spectroscopy of Supported PtMobimetallic Clusters. 1 - Experimental Technique. *J. Phys. Chem.*, **92**, 3542.

154 Samant, M.G., Bergeret, G., Meitzner, G., Gallezot, P. Boudart, M. (1988) Anomalous Wide Angle X-Ray Scattering and X-Ray Absorption Spectroscopy of Supported PtMo Bimetallic Clusters. 2 - Atomic and Electronic structure. *J. Phys. Chem.*, **92**, 3547.

155 Liang, K.S., Chien, F.Z., Hughes, G.J., Meitzner, G.D. and Sinfelt, J.H. (1991) The Nature of Rhenium in Silica Supported PtRe Clusters: Synchrotron X-Ray Diffraction Studies. *J. Phys. Chem.*, **95**, 9974.

156 Bellotto, M., Rebours, B., Clause, O., Lynch, J., Bazin, D. and Elkaim, E. (1996) Hydrotalcite Decomposition Mechanism: A Clue to the Structure and Reactivity of Spinel-like Mixed Oxides. *J. Phys. Chem.*, **100**, 8535.

157 Bellotto, M., Rebours, B., Clause, O., Lynch, J., Bazin, D. and Elkaim, E. (1996) A Reexamination of Hydrotalcite Crystal Chemistry. *J. Phys. Chem.*, **100**, 8527.

158 Bouchet-Fabre, B., Laruelle, S. and Figlarz, M. (1995) Awaxs Study of Amorphous WO_3 and $WO_3 \cdot nH_2O$. *NIMB*, **97**, 180.

159 Creux, S., Bouchet-Fabre, B. and Gaskell, P.H. (1995) Anomalous Wide Angle X-Ray Scattering Study of Strontium Silicate and Aluminosilicate Glasses. *Journal of Non-Crystalline Solids*, **192**, 360.

160 Bazin, D. and Revel, R. (1999) Improvement in the Structural Characterization of Nanometer Scale Metallic Oxide. The Xas-Awaxs Combined Approach. *J. Syn. Rad.*, **6**, 483.

161 Waseda, Y. (1984) *Novel Application of Anomalous (resonance) X-Ray Scattering for Structural Characterization of Disordered Material*, Ed. Springer-Verlag, Series: Lecture Notes in Physics, **204**.

162 Materlik, G., Sparks, C.J. and Fisher, K. (1994) *Resonant Anomalous X-Ray Scattering*, Ed. North Holland.

163 Stuck, J.B., Raoux, D., Chieux, P. and Riekel, C. (1993) Methods in the Determination of Partial Structure Factors, Ed. World Scientific.

164 Bergeret, G. and Gallezot, P. (1993) In *Détermination de la structure atomique des catalyseurs solides par diffffraction des rayons X*, Ed. Dunod.

165 Gnutzmann, V. and Vogel, W. (1990) Structural Sensitivity of the Standard Platinum/Silica Catalyst EuroPt-1 to Hydrogen and Oxygen Exposure by *In Situ* X-Ray Diffraction. *J. Phys. Chem.*, 94, 4991.

166 Sasaki, S. (1983) *KEK Report 83-82*, Nat. Lab. for High Energy Physics, Tsukuba, Japan.

Final manuscript received in October 2003